Chinese Chemical Letters 34 (2023) 108080

Contents lists available at ScienceDirect

Chinese Chemical Letters

journal homepage: www.elsevier.com/locate/cclet

# Protonic recognition and assembly for the creation of porous Brønsted acid catalysts with enhanced catalytic efficiency

Liping Huang[a,c,1], Mingyun Liang[a,1], Yajun Fang[a,1], Jehan Kim[d], Yuntian Yang[a], Zhegang Huang[a,b,*]

[a] PCFM, LIFM Lab, School of Chemistry, Sun Yat-sen University, Guangzhou 510275, China
[b] Guangdong Provincial Key Laboratory of Optical Chemicals, Xinhuayue Group, Maoming 525000, China
[c] Shenzhen Grubbs Institute, Department of Chemistry, Southern University of Science and Technology, Shenzhen 518055, China
[d] Pohang Accelerator Laboratory, Postech, Pohang, Gyeongbuk, Korea

ARTICLE INFO

*Article history:*
Received 30 June 2022
Revised 14 December 2022
Accepted 15 December 2022
Available online 18 December 2022

*Keywords:*
Tubular Brønsted acid
Protonic recognition
Dynamic assembly
Heterogeneous catalysis
Large-scale synthesis

ABSTRACT

Due to the high local concentration of substrates in confined space, porous solid Brønsted acids have been extensively explored for efficient acid-catalyzed reaction. However, the porous structures with strong Brønsted acids lack long-term stability due to chemical hydrolysis. Moreover, the products inhibition effect in confined rigid cavities severely obstructs subsequent catalysis. Here, tubular Brønsted acid catalyst with unique recognition of protons was presented by self-assembly of pH-responsive aromatic amphiphiles. The responsive assembly could mechanically transfer hydrogen ions from low-concentration acidic solution into tubular defined pores, thereby producing effective catalytic activity for Mannich reactions in mildly acidic solution. Notably, the tubular catalyst unfolded into flat sheets upon addition of triethylamine for efficient release of products, which could be recovered by subsequent acidification and the catalytic activity still remained. Therefore, the porous Brønsted acid with reversible assembly provides a new strategy for mass synthesis through increasing conversion times.



Brønsted acid catalysis is of great significance in the synthesis of pharmaceuticals and fine chemicals [1,2]. Although various liquid acids such as HCl, $H_2SO_4$, and HF have been widely used as homogeneous catalysts and exhibited efficient catalytic performance, the limitation of effective collision between bulk reagents has been a serious problem for the efficient catalysis in diluted solution [3]. In this regard, introduction of Brønsted acids into porous supporting materials, such as zeolites [4,5], mesoporous silicon [6,7], carbon [8,9], polymers [10,11], metal organic cages (MOCs) [12,13], metal organic frameworks (MOFs) [14,15] and covalent organic frameworks (COFs) [16,17], is a promising alternative to traditional homogeneous acids. However, most porous catalysts are labile with the treatment of strong acids, which exhibit poor stability and recyclability [18]. Despite the presence of stable porous catalysts, the rigid and robust pores are easily occupied by bulk products during the process of reaction for steady interaction, which seriously prevents the subsequent effective catalysis due to the products inhibition in confined cavities [19].

Mechanically uptaking reagents to substitute products in hollow aperture through dynamic assembly of catalytic device is a promising solution for this challenging problem [20]. Up to now, various strategies for the construction of dynamic catalysts have been exploited by external stimuli such as pH [21], solvent [22], temperature [23] and light [24] to realize spontaneous release of products through structural collapse based on regulable noncovalent interactions, but the soft catalysts from weak noncovalent interactions are too delicate to use as efficient Brønsted acid catalysts for the lack of long-term stability by the treatment of strong acids [25]. Among the self-assembled systems, aromatic rod amphiphiles composed of conjugated carbon and hydrophilic dendritic segments can easily aggregate into porous structures with hydrophobic characteristics, which are well suitable as defined scaffolds for organic synthesis [26,27]. In addition, compared to traditional rigid pores obtained from strong Brønsted acids, the acidification of porous materials based on aromatic rod assembly can be achieved in mildly acidic environment through the chemical treatment of aromatic rod blocks [28]. For example, introduction of methoxy group at the ortho-position of 2,6-biphenyl pyridine would increase the alkalinity behavior for the formation of fused triad [29]. As hinted from the special proton recognition of aromatic segment, here we

* Corresponding author.
*E-mail address:* huangzhg3@mail.sysu.edu.cn (Z. Huang).
[1] These authors contributed equally to this work.

https://doi.org/10.1016/j.cclet.2022.108080
1001-8417/

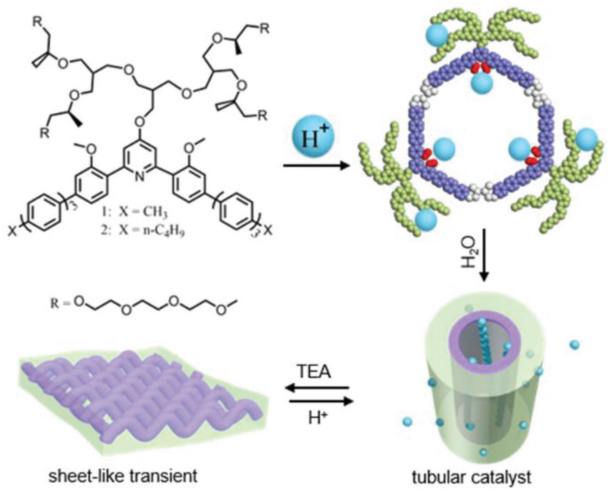


**Fig. 1.** Chemical structures, protonic recognition and dynamic assembly of bent-shaped triblock amphiphiles.

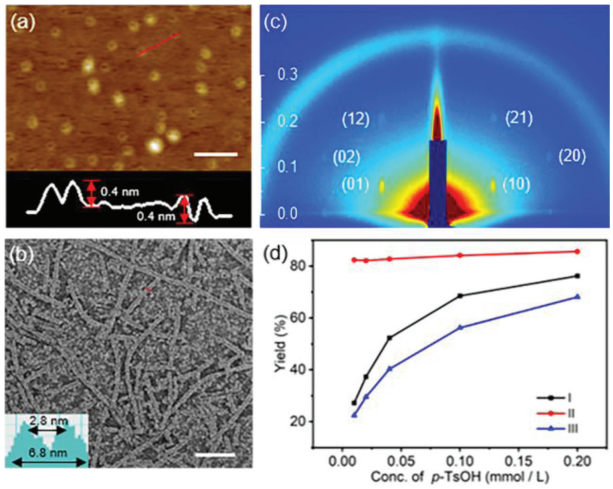


**Fig. 2.** (a) AFM height image of toroidal aggregation from 10 mmol/L acetone solution of **2** with 2 equiv. *p*-TsOH. (b) TEM image of tubular Brønsted acid catalysts from 0.1 mmol/L aqueous solution of **2** with 2 equiv. *p*-TsOH. (c) 2D XRD pattern of tubular aggregation from 0.1 mmol/L aqueous solution of **2** with 2 equiv. *p*-TsOH, y axis is *q* space ($Å^{-1}$). (d) *p*-TsOH concentration-dependent catalytical behavior for Mannich reaction with 0.2 $\mu$mol $R_1$, $R_2$ and $R_3$ in homogeneous ethanol solution (I), aqueous dispersion with tubular supporter of **2** (2.5 mol%) (II) and acetone solution with toroidal supporter of **2** (2.5 mol%) (III), more details see Table S1. Both scale bars in (a) and (b) are 50 nm.

propose a unique tubular Brønsted acid catalyst by the assembly of tri-block aromatic amphiphiles. Recently, we have extended the pH-sensitive aromatic block into 120°-folded aromatic amphiphiles to realize special recognition of protons in dilute acidic solution, which resulted in the lateral aggregation to form hexameric toroids [30]. The toroidal nanostructures based on the assembly of hydrophilic amphiphiles could easily connect with each other to form porous tubules by the enhanced hydrophobicity [31]. As hinted from the formation of tubular space confinement, here we tried to align acidified cyclic aggregation to prepare tubular Brønsted acid catalyst. Depending upon the specific recognition, the hydrogen ions could be transferred from low-concentration acidic solution into the inner wall of tubules through structural turnover of aromatic segments. Remarkably, the assembled tubules with concentrated acidic environment exhibited excellent catalytic performance and long-term stability towards Mannich reaction. Unlike solid Brønsted catalysts, the tubular catalyst was able to expand into flat sheets by deprotonation and spontaneously release products, which could be recovered by subsequent acidification and the catalytic efficiency still remained. Thus, the mass synthesis was achieved by the tubular catalysts with dynamic assembly through increasing conversion times (Fig. 1).

To prepare tubular Brønsted acid based on the stacking of acidified cyclic aggregates, we have introduced the hydrophobic alkyl segments into the hole of cyclic aggregates through the assembly of bent-shaped triblock amphiphiles. The self-association of cyclic aggregation was determined by increasing the length of terminal alkyl chain from the self-assembly of designed triblock amphiphiles. Both triblock amphiphiles **1** and **2** were soluble in polar organic solvent such as acetone. However, the addition of *p*-toluenesulfonic acid (*p*-TsOH) into acetone solution drove **2** with butyl terminal to self-assemble into nanostructures. Upon addition of *p*-TsOH, the amphiphile showed red-shifted absorption and enhanced fluorescence relative to that observed in acetone solution (Fig. S2 in Supporting information), suggesting the formation of *J*-type aggregation by acidification [32]. Indeed, the transmission electron microscopy (TEM) with negatively stained samples from 10 mmol/L acetone solution with 2 equiv. *p*-TsOH showed toroidal objects with a diameter of 6.8 nm and an internal cavity of 2.8 nm (Fig. S3a in Supporting information). When the acidic solution was cast onto mica, the atomic force microscopy (AFM) revealed uniform toroidal objects with the height of 0.4 nm (Fig. 2a), demonstrating that the toroids were unilaminar macrocycle. Interestingly, the addition of water into toroidal solution would trigger larger aggregates, which was reflected in the increased hydrodynamic diameter from 16 nm to 268 nm in dynamic light scattering (DLS) (Fig. S3b). TEM with negatively stained samples from 0.1 mmol/L aqueous solution gave that the toroids transformed into hollow tubular aggregation with an external and inner diameter of 6.8 nm and 2.8 nm (Fig. 2b). The observed diameters of the tubules were identical with those of original toroids, suggesting that the tubules were formed by toroidal stacking. To further understand tubular formation, the 1D objects were successfully aligned and transformed onto thin films to perform two-dimensional X-ray diffraction (2D XRD). The sample of **2** displayed 2D ordered patterns with the ratio of $1:\sqrt{3}:2$ at the small-angle range, which could be assigned as 2D hexagonal columnar structures with corresponding lattice parameters of 4.8 nm (Fig. 2c). On the basis of these results and measured density, the number of molecules in monolayer unit cell could be calculated as three, suggesting that the tubular aggregates were based on the stacking of trimeric toroidal aggregates [33]. To gain insight into the packing arrangement of the aromatic segments within hollow aggregation, the proton nuclear magnetic resonance ($^1$H NMR) was performed with the toroidal objects in deuterated acetone. The $^1$H NMR of **2** showed that most of the protons in pyridine and anisole segments were downfield shifted except the proton ortho to pyridine (Ho) through the formation of toroidal aggregation by trifluoroacetic (TFA) titration (Fig. S4 in Supporting information), indicating the formation of hydrogen bonding in pyridine and methoxy segments within trimeric cyclic aggregates. Notably, the Ho proton facing to nitrogen in neutral state was gradually up-field shifted even in the reduced shielding effect by $NH^+$ group, suggesting the Ho moved away from the $NH^+$ group through rotation of $C_{Py}$-$C_{Ph}$ bond [29]. These observations indicated that protons were transferred from acidic dilution into the inner hole of trimeric toroidal aggregates upon addition of TFA, which in turn stacked on top of each other to form the porous tubules.

Owing to the existence of concentrated proton environment in tubular pores, the tubules can be employed as efficient Brønsted acid catalysts. Accordingly, Mannich reaction with benzaldehyde, phenylamine and acetophenone was catalyzed by tubular catalysts

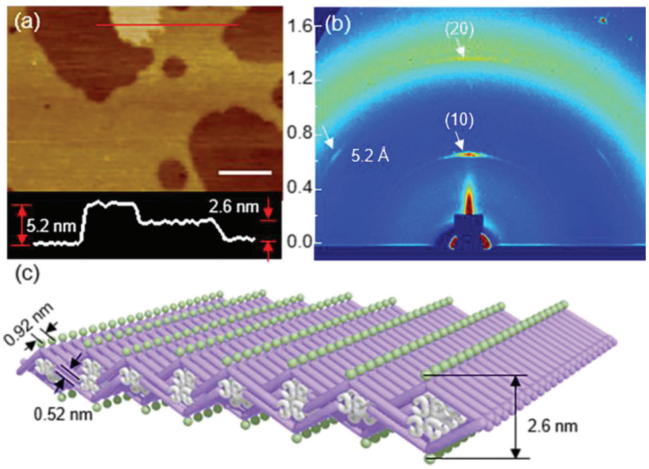


**Fig. 3.** AFM height image (a) and 2D-XRD pattern (b) of sheet-like transient aggregates of **2** from 0.1 mmol/L deprotonated aqueous solution by the addition of 3 equiv. TEA, scale bar of (a) is 500 nm, y axis of (b) is $q$ space ($Å^{-1}$). (c) Sheet-like transient state from alternative stacking of zigzag aggregation.

in aqueous solution and corresponding homogeneous catalysts *p*-TsOH in ethanol as a comparison [34]. As shown in Fig. 2d and Table S1 (Supporting information), the catalytic performance was obviously dependent on the concentration of *p*-TsOH in ethanol solution since the concentrated proton was conducive to the formation of stable imine intermediate [35]. In contrast to homogeneous catalysts, the tubular catalysts based on the aqueous assembly of **2** showed remarkably high catalytic efficiency even in the mildly acidic environment, indicating that the high catalytic behavior of tubular catalysts was attributable to its well-defined hollow space. To take insight into the catalytic effect of defined pores, the toroidal catalyst of **2** in acetone was used for control experiment. Although the toroidal supporter possessed protonated hollow environment, it did not show an enhanced catalytic effect for Mannich reaction, proving that the protonated hollow environment in combination with space confinement was indispensable to efficient catalysis [36,37]. The promotion of the reaction within confined protonated pores of catalyst **2** was also observed for series of substrates with different substituent groups, which demonstrated tubular Brønsted acid catalyzer was applicable to various reactants for Mannich reaction (Table S2 in Supporting information). In addition, the tubular catalysts based on the self-assembly of aromatic triblock amphiphiles exhibited significant chemical stability in strong acid solution for the effective separation of aromatic skeletons from acidic environment by hydrophilic ethylene oxide segments. After treatment with HCl (pH 2) solution at 30 °C for two weeks, the tubular morphologies remained unchanged (Fig. S5 in Supporting information). Nonetheless, the catalytic efficiency of tubular catalysts was obviously reduced with the bulky substrates due to the blocking of porous cavity (Table S2).

We noticed that the deprotonation would generate the opening of folded tubular catalysts through increased $\pi$-$\pi$ stacking, resulting in spontaneous release of products. After treatment of tubular solution with TEA, the solution showed blue-shifted absorption and significantly quenched fluorescence (Fig. S6 in Supporting information), suggesting that the slipped *J*-type aggregation based on the stacking of trimeric macrocycles changed into fully overlapped *H*-type assembly. Remarkably, TEM and AFM showed thin layers with the thickness of 2.6 nm, close to the observed wall thickness of tubular catalysts (Fig. 3a and Fig. S7 in Supporting information), indicating that the tubular catalysts were triggered to unfold into layered structure through *H*-type stacking. To identify the molecular packing in the thin lamina, 2D-XRD experiment was further performed. The film of **2** from slow evaporation of alkaline solution displayed two equidistant diffractions (10) and (20) with a spacing of 9.2 Å in vertical direction (Fig. 3b). Considering approximate $\pi$-$\pi$ stacking distance between neighboring aromatic segments, the equal spacing was two times as large as $\pi$-$\pi$ stacking, indicating that the layered structure arose from the alternative stacking of infinite thin tetragonal plate with the width of 2.6 nm. Furthermore, the wide angle scattering exhibited two identical diffractions with d spacing of 5.2 Å along to the (10) direction. This result revealed the aromatic segments adopted a zigzag conformation to generate infinite tetragonal planes with the hydrophobic alkyl segments

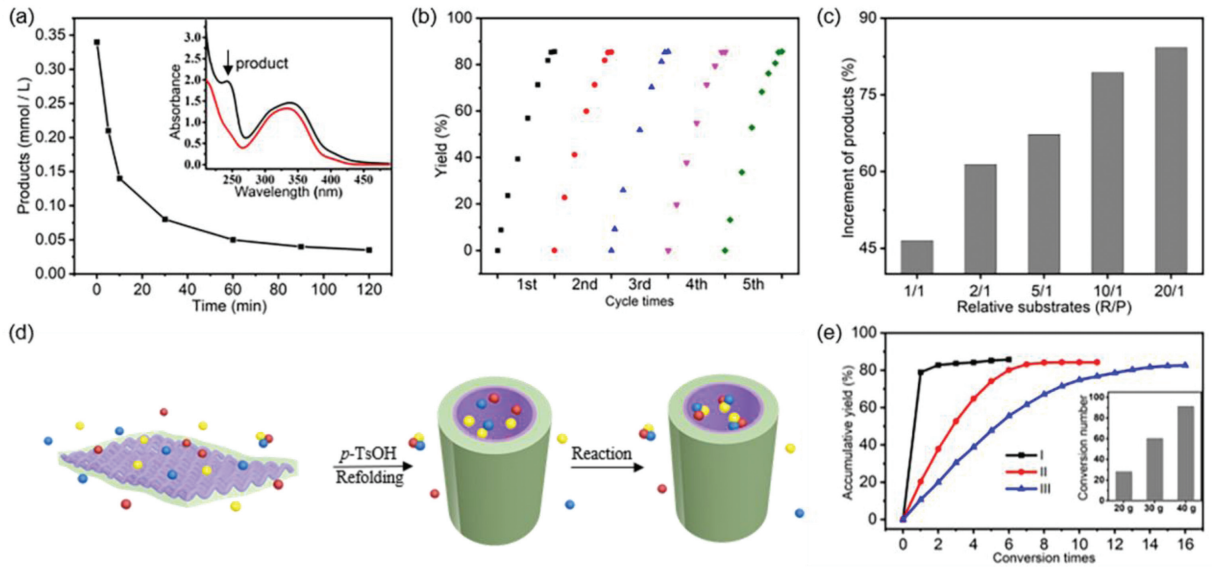


**Fig. 4.** (a) Release profile of products from tubular catalysts after treating with TEA, the insert is corresponding absorption spectra before (black line) and after (red line) the release of products. (b) Real-time catalytic yield in five cycle reactions. (c) Enhanced catalytic behavior of tubular catalyst **2** through efficiently encapsulating reagents with increasing ratios of reagents/products during regeneration from sheet-like transient state. (d) Schematic representation of the selective encapsulation of more reagents than products through refolding of sheet-like transient state, red, yellow and blue balls stand for reagent $R_1$, $R_2$ and $R_3$ while the combination of red, yellow and blue balls represents product. (e) The accumulative yields for the synthesis 1 g (I), 5 g (II), and 10 g (III) with 0.2 g tubular Brønsted acid catalysts **2** through increasing conversion times and the insert is the corresponding conversion times for the large scale synthesis.

inside, which were further aggregated in one dimension with an ABAB arrangement to form 2D thin lamina (Fig. 3c).

Importantly, the unfolding of tubular catalysts by deprotonation facilitated the release of products. Owing to the poor diffusion of products in alkaline solution, the bulky products were spontaneously precipitated and separated from layered substrates (Fig. 4a). Thus, the porous catalysts were readily recovered by subsequent acidification after completing release of the products and reused upon addition of new reactants. The recycling procedures revealed that the initial catalytic efficiency was completely maintained during 5 cycles (Fig. 4b).

The regeneration of catalytic capability through dynamic assembly motivated us to explore the advanced porous acid catalysts for large-scale synthesis through increasing conversion times. When there were more reagents than products in solution, the refolding of sheet-like transient after one cyclic reaction would generate the efficient exchange of products and reagents to ensure subsequent catalysis. With this in mind, we initially investigated different ratios of reagents with a certain amount of products to confirm the selective encapsulation in the refolding process. As shown in Fig. 4c, the products gradually increased with increasing ratios of reagents/products upon addition of *p*-TsOH into layered supporter, demonstrating that during regeneration the tubular catalysts tended to encapsulate excessive substrates to promote next reaction (Fig. 4d). Thus, by virtue of the unique uptaking behavior, tubular catalysts could achieve large-scale synthesis through reversible assembly (Fig. S9 in Supporting information). The conversion in each cyclic reaction was monitored as shown in Fig. 4e. Although the catalytic yield gradually decreased with increasing conversion times, the accumulative reaction efficiency was nearly close to initial level.

In summary, we have constructed stable tubular Bronsted catalysts with protonic recognition in mildly acidic solution from assembly of triblock amphiphiles. The tubular catalysts could transfer hydrogen ions successfully from dilute aqueous solution into separated tubular wall to promote the acid catalysis. Due to the decoration by hydrophilic oligoether dendrons, the confined tubular pores were effectively separated from aqueous environment and thus exhibited remarkable chemical stability even in strong acidic solution. In contrast to traditional porous Brønsted acid catalysts that were easily blocked by products, the presented tubular Brønsted acid catalyst could transform into sheet-like transient state upon addition of TEA, inducing the spontaneous release of products. Subsequently, the tubular catalysts were able to recover with initial catalytic efficiency by acidification. In addition, the refolded tubules from sheet-like transient tended to encapsulate more reagents than products, facilitating the subsequent catalysis. Therefore, the construction of tubular Brønsted acid catalysts with reversible assembly provides a new strategy of large-scale synthesis through increasing conversion times.

## Declaration of competing interest

The authors declare that they have no known competing financial interests or personal relationships that could have appeared to influence the work reported in this paper.

## Acknowledgments

This work was supported by the Natural Science Foundation of China (No. 21871299), Guangdong Natural Science Funds for Distinguished Young Scholar (No. 2019B151502051), the Fundamental Research Funds for the Central Universities (No. 19lgzd21), Guangdong Basic and Applied Basic Research Foundation (No. 2022A1515110991) and China Postdocroral Science Foundation (No. 2021M701569). We thank the Open Project of State Key Laboratory of Supramolecular Structure and Materials (Jilin University), and the Key Laboratory of Functional Inorganic Material Chemistry (Heilongjiang University).

## Supplementary materials

Supplementary material associated with this article can be found, in the online version, at doi:10.1016/j.cclet.2022.108080.

## References

[1] J. Yu, F. Shi, L.Z. Gong, Acc. Chem. Res. 44 (2011) 1156–1171.
[2] Z.L. Xia, Q.F. Xu-Xu, C. Zheng, S.L. You, Chem. Soc. Rev. 49 (2020) 286–300.
[3] F. Liu, K. Huang, A. Zheng, F.S. Xiao, S. Dai, ACS Catal. 8 (2018) 372–391.
[4] Y. Guefrachi, G. Sharma, D. Xu, et al., Angew. Chem. Int. Ed. 59 (2020) 9579–9585.
[5] T.H. Chen, D.G. Vlachos, S. Caratzoulas, ACS Catal. 11 (2021) 9916–9925.
[6] Q. Yue, M. Wang, J. Wei, et al., Angew. Chem. Int. Ed. 51 (2012) 10368–10372.
[7] Q. Wu, F. Liu, X. Yi, Y. Zou, L. Jiang, Green Chem. 20 (2018) 1020–1030.
[8] K. Nakajima, M. Hara, ACS Catal. 2 (2012) 1296–1304.
[9] S. Xiong, C. Luo, Z. Yu, et al., Green Chem. 23 (2021) 8458–8467.
[10] Q. Sun, S. Wang, B. Aguila, et al., Nat. Commun. 9 (2018) 3236.
[11] Q. Sun, K. Hu, K. Leng, et al., J. Mater. Chem. A 6 (2018) 18712–18719.
[12] C. Ngai, C.M. Sanchez-Marsetti, W.H. Harman, R.J. Hooley, Angew. Chem. Int. Ed. 59 (2020) 23505–23509.
[13] D. Chu, W. Gong, H. Jiang, et al., CCS Chem. 3 (2021) 1692–1700.
[14] L. Feng, Y. Wang, S. Yuan, et al., ACS Catal. 9 (2019) 5111–5118.
[15] W. Gong, Y. Liu, H.Y. Li, Y. Cui, Coordin. Chem. Rev. 420 (2020) 213400.
[16] Q. Sun, Y. Tang, B. Aguila, et al., Angew. Chem. Int. Ed. 58 (2019) 8670–8675.
[17] B. Hou, S. Yang, K. Yang, et al., Angew. Chem. Int. Ed. 60 (2021) 6086–6093.
[18] D. Yang, B. Gates, ACS Catal. 9 (2019) 1779–1798.
[19] A.B. Grommet, M. Feller, R. Klajn, Nat. Nanotechnol. 15 (2020) 256–271.
[20] S. Wu, L. Huang, Y. Hou, et al., Commun. Chem. 3 (2020) 11.
[21] C. Edlinger, T. Einfalt, M. Spulber, et al., Nano Lett. 17 (2017) 5790–5798.
[22] X. Zhang, Y. Zhao, S. Xu, et al., Nat. Commun. 5 (2014) 3170.
[23] R. Borrmann, V. Palchyk, A. Pich, M. Rueping, ACS Catal. 8 (2018) 7991–7996.
[24] H. Zhao, S. Sen, T. Udayabhaskararao, et al., Nat. Nanotechnol. 11 (2016) 82–88.
[25] L.R. Holloway, P.M. Bogie, Y. Lyon, et al., J. Am. Chem. Soc. 140 (2018) 8078–8081.
[26] H. Wang, Y. Wang, B. Shen, X. Liu, M. Lee, J. Am. Chem. Soc. 141 (2019) 4182–4185.
[27] X. Liu, X. Zhou, B. Shen, et al., J. Am. Chem. Soc. 142 (2020) 1904–1910.
[28] Y. Kim, H. Li, Y. He, et al., Nat. Nanotechnol. 12 (2017) 551–556.
[29] J. Leblond, H. Gao, A. Petitjean, J.C. Leroux, J. Am. Chem. Soc. 25 (2010) 8544–8545.
[30] L. Huang, H. Zhang, S. Wu, et al., iScience 19 (2019) 224–231.
[31] E. Lee, J.K. Kim, M. Lee, J. Am. Chem. Soc. 131 (2009) 18242–18243.
[32] F. Wurthner, T.E. Kaiser, C.R. Saha-Moller, Angew. Chem. Int. Ed. 50 (2011) 3376–3410.
[33] Z. Huang, J.H. Ryu, E. Lee, M. Lee, Chem. Mater. 19 (2007) 6569–6574.
[34] S. Iimura, D. Nobutou, K. Manabe, S. Kobayashi, Chem. Commun. (2003) 1644–1645.
[35] J. Hine, J.C. Craig, J.G. Underwood II, F.A. Via, J. Am. Chem. Soc. 92 (1970) 5194–5199.
[36] V. Mouarrawis, R. Plessius, J.I. van der Vlugt, J. N. H. Reek, Front. Chem. 6 (2018) 623.
[37] J. Dai, H. Zhang, Small 17 (2021) 2005334.